

Long afterglow $\text{SrAl}_2\text{O}_4\text{:Eu,Dy}$ phosphors for CdS quantum dot-sensitized solar cells with enhanced photovoltaic performance

Cite this: *J. Mater. Chem. A*, 2013, **1**, 6388

Hengchao Sun, Likun Pan,* Xianqing Piao and Zhuo Sun

An efficient bifunctional structured layer composed of long afterglow $\text{SrAl}_2\text{O}_4\text{:Eu,Dy}$ phosphors on top of a transparent layer of nanocrystalline TiO_2 was fabricated for use in CdS quantum dot-sensitized solar cells (QDSSCs). The introduction of $\text{SrAl}_2\text{O}_4\text{:Eu,Dy}$ increases the photocurrent of the QDSSCs mainly due to enhanced light harvesting abilities via improved light absorption and scattering. Under one sun illumination (AM 1.5G, 100 mW cm^{-2}), cells containing $\text{SrAl}_2\text{O}_4\text{:Eu,Dy}$ show a marked improvement in their conversion efficiency (1.24%) compared with cells without $\text{SrAl}_2\text{O}_4\text{:Eu,Dy}$ (0.98%). After one sun illumination for 1 min, after which the light source was turned off, cells containing $\text{SrAl}_2\text{O}_4\text{:Eu,Dy}$ show an efficiency of 0.07% under dark conditions due to the irradiation by the long persistent light from $\text{SrAl}_2\text{O}_4\text{:Eu,Dy}$. The present strategy should provide a possibility to fulfil the operation of solar cells even in the dark.

Received 7th February 2013
Accepted 19th March 2013

DOI: 10.1039/c3ta10596b

www.rsc.org/MaterialsA

Introduction

Quantum dot-sensitized solar cells (QDSSCs) are considered as promising candidates for the development of next generation solar cells because they can be fabricated by simple and low-cost techniques.^{1–9} Despite the powerful merits of quantum dot (QD) materials, such as a high extinction coefficient, spectra tunability based on particle size and a good stability, the power conversion efficiency of a QDSSC is still low compared to that of a dye-sensitized solar cell (DSSC).^{10–20} Pursuing high efficiency is always a core task in the development of QDSSCs, and one of the current key issues is to enhance light harvesting abilities in the visible light region.^{21–25}

It is known that conventional semiconductor photoanodes, typically TiO_2 , which are composed of small nanoparticles with a size of 10–30 nm are transparent to solar light and can not effectively utilize the incident light.^{26–28} Therefore, an efficient light scattering layer, involving large ZnO, TiO_2 or ZrO particles such as aggregates, spherical structures, porous beads and nanoplates, on a TiO_2 layer has been suggested as one effective method to localize the incident light within an electrode and enhance light absorption by increasing the optical path length.^{29–36} Recently, the utilization of light-converting materials has been another attractive strategy to improve light harvesting abilities. These light-converting materials, including up-converting and down-converting materials, could transform lower (higher) energy photons into high (low)-energy visible

photons which are easily absorbed by the sensitizer.^{37–41} Hafez *et al.*⁴² reported that the use of Sm^{3+} -doped and Eu^{3+} -doped TiO_2 electrodes in DSSCs improved the conversion efficiency due to their down-converting properties. In our previous work, a bifunctional structured layer composed of $\text{Y}_3\text{Al}_5\text{O}_{12}\text{:Ce}$ phosphors on top of a TiO_2 layer was used in DSSCs and the cells achieved an improved efficiency due to the light scattering and the light down-converting properties of the phosphors.⁴³

In this work, we further study an efficient bifunctional structured layer composed of $\text{SrAl}_2\text{O}_4\text{:Eu,Dy}$ phosphors that offer both light scattering and light down-converting properties on top of a TiO_2 layer for use in QDSSCs. It is known that $\text{SrAl}_2\text{O}_4\text{:Eu,Dy}$ is a long afterglow phosphor, which not only acts as a down-converting material, but also exhibits the excellent luminescent property of long persistence.^{44,45} Under one sun illumination, cells containing $\text{SrAl}_2\text{O}_4\text{:Eu,Dy}$ show a marked improvement in their conversion efficiency (1.24%) compared to cells without $\text{SrAl}_2\text{O}_4\text{:Eu,Dy}$ (0.98%). Importantly, the $\text{SrAl}_2\text{O}_4\text{:Eu,Dy}$ phosphors still emit light to drive the QDSSCs even if the light source is turned off after illumination.

Experimental

A transparent layer of nanocrystalline TiO_2 (P25, Degussa) with a thickness of *ca.* 10 μm was prepared by screen printing P25 paste onto F-doped SnO_2 (FTO) (resistivity: $14 \Omega \square^{-1}$, Nippon Sheet Glass, Japan) glass. Subsequently, the $\text{SrAl}_2\text{O}_4\text{:Eu,Dy}$ phosphors (Jinan Xingyue LED Technology Co., Ltd.) were deposited on top of a TiO_2 layer by screen printing. The as-prepared electrodes were sintered at 500 $^\circ\text{C}$ for 30 min.

Engineering Research Center for Nanophotonics & Advanced Instrument, Ministry of Education, Department of Physics, East China Normal University, Shanghai, China.
E-mail: lkpan@phy.ecnu.edu.cn; Fax: +86 21 62234321; Tel: +86 21 62234132

The electrodes were then sensitized by CdS QDs using a microwave-assisted chemical bath deposition method as reported in our previous work.^{7,46,47} In brief, the electrodes were immersed into a sealed vessel with a CdS precursor aqueous solution (0.05 M $\text{Cd}(\text{NO}_3)_2$ and 0.05 M $\text{CH}_4\text{N}_2\text{S}$, Sinopharm Chemical Reagents Co. Ltd.). Then, the vessel was put into an automated focused microwave system (Explorer-48, CEM Co.) and treated at 150 °C with a microwave irradiation power of 100 W for 20 min.

The CdS QDSSCs were sealed in a sandwich structure with a 60 μm spacer (Surlyn) using a thin Pt counter electrode. A water/methanol (3 : 7 by volume) solution was used as a co-solvent for the polysulfide electrolyte. The electrolyte solution consists of 0.5 M Na_2S , 2 M S, and 0.2 M KCl.⁴⁸ The active area of the cells is 0.2 cm^2 .

The surface morphology and composition of the electrodes were characterized by field-emission scanning electron microscopy (FESEM, Hitachi S-4800) and energy dispersive X-ray spectroscopy (EDS, JEM-2100). UV-vis diffuse reflection and absorption spectra of the electrodes were detected using a UV-vis spectrophotometer (Hitachi U-3900). Photoluminescence (PL) spectra were examined using a fluorescence spectrophotometer (HORIBA Jobin Yvon fluoromax-4). A J - V measurement was performed using a Keithley model 2440 Source Meter and a Newport solar simulator system (equipped with a 1 kW xenon arc lamp, Oriel) at one sun ($\text{AM } 1.5\text{G}$, 100 mW cm^{-2}) with a mask. The incident photon to current conversion (IPCE) efficiency was measured as a function of wavelength from 300 to 600 nm using an Oriel 300 W xenon arc lamp and a lock-in amplifier M 70104 (Oriel) under monochromator illumination. An electrochemical impedance spectroscopy (EIS) measurement was performed using an electrochemical workstation (AUTOLAB PGSTAT302N) under 100 mW cm^{-2} illumination in the frequency range of 0.1 Hz–100 kHz, and the applied bias voltage and ac amplitude were set at the open-circuit voltage of the cells and 10 mV between the counter electrode and the working electrode, respectively.

Results and discussion

Fig. 1a and b show FESEM images of the P25 and P25/ $\text{SrAl}_2\text{O}_4\text{:Eu,Dy}$ electrodes, respectively. As illustrated in Fig. 1a, the pure P25 electrode consists of a random agglomeration of TiO_2 particles. Compared with pure P25, it is observed that the $\text{SrAl}_2\text{O}_4\text{:Eu,Dy}$ phosphors are deposited on the surface of the TiO_2 film (Fig. 1b). The $\text{SrAl}_2\text{O}_4\text{:Eu,Dy}$ phosphor particles have sizes in the range of 5–10 μm . Fig. 1c displays the FESEM image of the P25/ $\text{SrAl}_2\text{O}_4\text{:Eu,Dy/CdS}$ electrode. An apparent difference in the surface morphology is observed compared with the P25/ $\text{SrAl}_2\text{O}_4\text{:Eu,Dy}$ electrode, indicating the successful attachment of the CdS QDs. The composition of the P25/ $\text{SrAl}_2\text{O}_4\text{:Eu,Dy/CdS}$ electrode was identified by an EDS measurement, as shown in Fig. 1d, which confirms the existence of TiO_2 , $\text{SrAl}_2\text{O}_4\text{:Eu,Dy}$ and CdS in the electrode.

The UV-vis diffuse reflection spectra of the P25 and P25/ $\text{SrAl}_2\text{O}_4\text{:Eu,Dy}$ electrodes are shown in Fig. 2a. It is observed that the P25/ $\text{SrAl}_2\text{O}_4\text{:Eu,Dy}$ electrode has a higher light reflectance

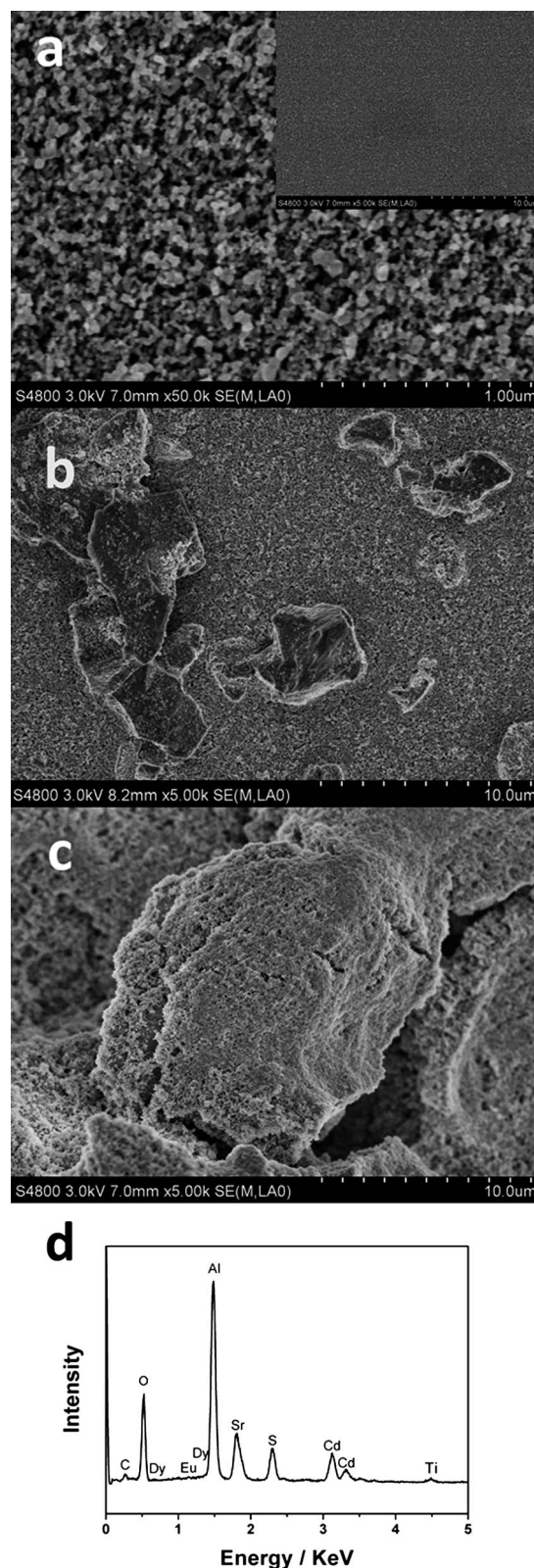


Fig. 1 The surface morphologies of the (a) P25 (inset is the low magnification image), (b) P25/ $\text{SrAl}_2\text{O}_4\text{:Eu,Dy}$ and (c) P25/ $\text{SrAl}_2\text{O}_4\text{:Eu,Dy/CdS}$ electrodes measured by FESEM. (d) The EDS spectrum for the P25/ $\text{SrAl}_2\text{O}_4\text{:Eu,Dy/CdS}$ electrode.

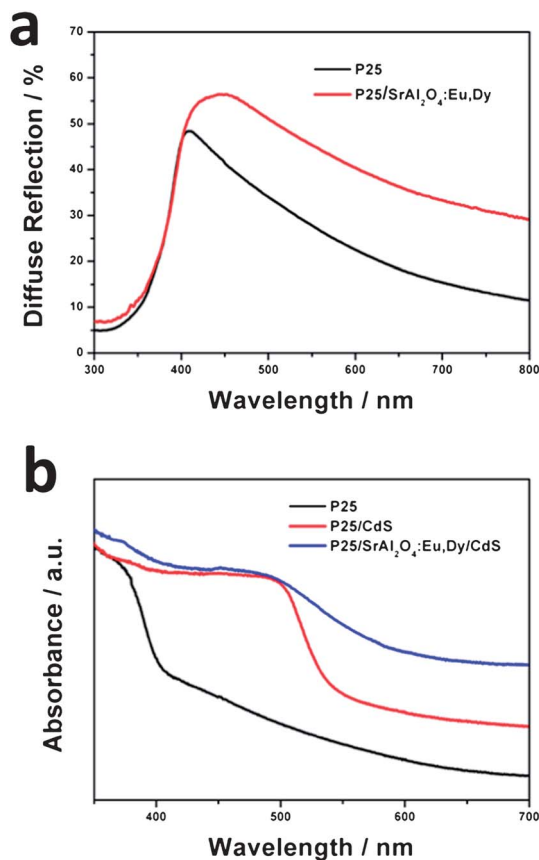


Fig. 2 (a) UV-vis diffuse reflectance spectra for the P25 and P25/SrAl₂O₄:Eu,Dy electrodes, (b) UV-vis absorption spectra for the P25, P25/CdS and P25/SrAl₂O₄:Eu,Dy/CdS electrodes.

than the bare P25 electrode, which indicates that the additional SrAl₂O₄:Eu,Dy phosphors improve the light scattering capabilities, resulting in an improved light harvesting ability. Fig. 2b displays the UV-vis absorption spectra of the P25, P25/CdS and P25/SrAl₂O₄:Eu,Dy/CdS electrodes. Compared with the absorption spectrum for the P25 electrode, there is an obvious absorption peak near 500 nm for the P25/CdS and P25/SrAl₂O₄:Eu,Dy/CdS electrodes, which is due to the contribution from CdS QDs.⁴⁶ It should be noticed that the P25/CdS and P25/SrAl₂O₄:Eu,Dy/CdS electrodes have a similar absorbance near 500 nm, indicating that the introduction of the large SrAl₂O₄:Eu,Dy particles only has a small influence on the amount of CdS deposited on the electrodes.

Fig. 3 shows the PL excitation and emission spectra for SrAl₂O₄:Eu,Dy. The absorption peak at 335 nm is assigned to the characteristic $4f^7 \rightarrow 4f^65d^1$ transition of the Eu²⁺ ions. A broad emission spectrum with a peak at 512 nm is observed, which is typical of the $4f^65d^1 \rightarrow 4f^7$ emission of the Eu²⁺ ions. This luminescence falls in the absorption range of the CdS QDs. Therefore, the result indicates that SrAl₂O₄:Eu,Dy can be used as an effective light down-converting material to improve light harvesting abilities in QDSSCs.⁴³ Furthermore, Dy³⁺ ions, as hole traps, play an important role in the long afterglow properties of SrAl₂O₄:Eu,Dy. When the excitation light source is turned off, some holes captured by the Dy³⁺ hole traps could be

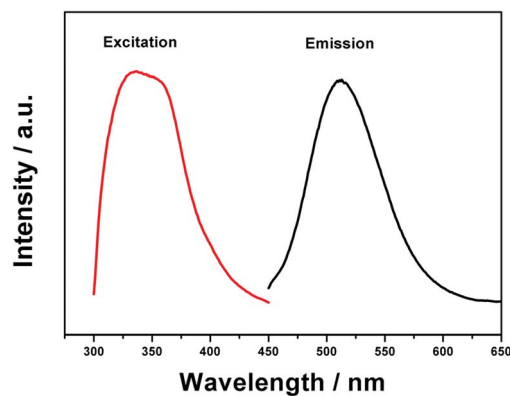


Fig. 3 PL excitation and emission spectra of SrAl₂O₄:Eu,Dy ($\lambda_{\text{ex}} = 335$ nm, $\lambda_{\text{em}} = 512$ nm).

thermally released slowly to valence bands. The released holes travel back to Eu²⁺, returning to the ground state of Eu²⁺ which is accompanied by light emission.^{44,45} Generally, the SrAl₂O₄:Eu,Dy phosphor is one of the best afterglow materials. The afterglow of this phosphor persists for a very long time after full illumination, and the green emission can be observed by the naked eye for several hours.^{49–51} Such a long persistent light can be considered to drive the solar cells in the dark, though its intensity still needs to be improved substantially.

The EIS spectra of the cells containing P25/CdS and P25/SrAl₂O₄:Eu,Dy/CdS electrodes are shown in Fig. 4.^{52,53} Two semicircles, including a small one at a high frequency and a large one at a low frequency, are observed in the Nyquist plots of the EIS spectra and the corresponding equivalent circuit is shown in the inset of Fig. 4a. The high frequency semicircle is related to the charge transfer resistance (R_{ct}) at the interface between the electrolyte and counter electrode. The larger semicircle at a low frequency is due to the contribution from the electron transport resistance (R_{w}) and the interfacial capacitance at the photoanode/electrolyte interface. The fitted R_{w} of the cells containing the P25/SrAl₂O₄:Eu,Dy/CdS electrode is lower than that of the cells containing the P25/CdS electrode, reflecting the acceleration of the electron transfer process in the photoanode. This result indicates favored electron transport and a reduction of the electron recombination when SrAl₂O₄:Eu,Dy is introduced.

The J - V curves of the cells containing the P25/CdS and P25/SrAl₂O₄:Eu,Dy/CdS electrodes are shown in Fig. 5a. The open circuit potential (V_{oc}), short circuit current density (J_{sc}), fill factor (FF) and conversion efficiency (η) of all the cells are listed in Table 1. It can be observed that the J_{sc} and η values have largely increased from 5.87 mA cm⁻² and 0.98% for cells containing the P25/CdS electrode to 7.07 mA cm⁻² and 1.24% for cells containing the P25/SrAl₂O₄:Eu,Dy/CdS electrode. The improvement in the J_{sc} and V_{oc} values results from the introduction of SrAl₂O₄:Eu,Dy into the QDSSCs. The reasons can be summarized as follows: (1) when the SrAl₂O₄:Eu,Dy phosphors are introduced into the photoanode, they can absorb higher energy photons and emit visible light at a longer wavelength, which has been confirmed by the PL spectra. These low energy

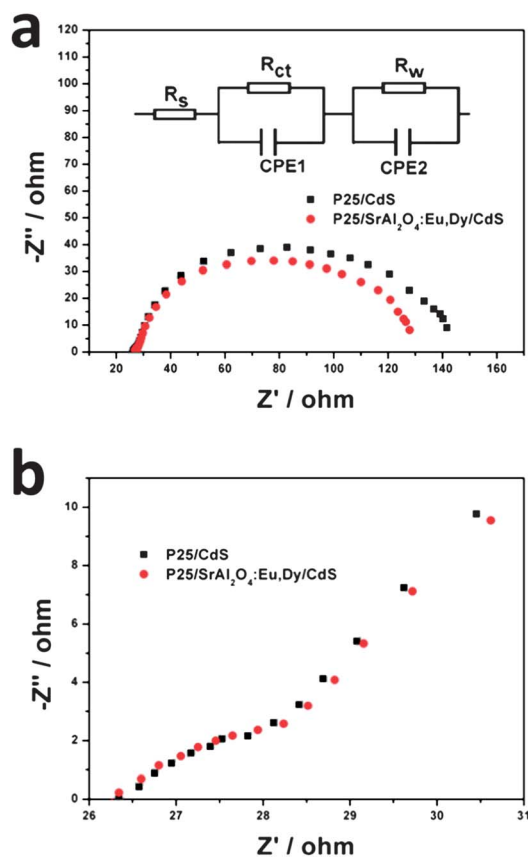


Fig. 4 (a) EIS spectra for the cells containing the P25/CdS and P25/SrAl₂O₄:Eu,Dy/CdS electrodes. The inset displays the corresponding equivalent circuit. (b) A magnification of the high frequency parts of the spectra.

photons can be easily absorbed by the CdS QDs, leading to an improvement in the conversion efficiency for the QDSSCs;^{37–43} (2) light scattering by the SrAl₂O₄:Eu,Dy phosphor particles enhances the light harvesting abilities of the cells, which has been confirmed from the UV-vis diffuse reflection spectra; (3) the introduction of SrAl₂O₄:Eu,Dy favors electron transfer and suppresses electron recombination, which has been confirmed by EIS measurements. The IPCE spectra show that cells containing the P25/SrAl₂O₄:Eu,Dy/CdS electrode exhibit a maximum IPCE value of 43.2% at 440 nm, while for cells containing the P25/CdS electrode, the peak only reaches 36.6%, as shown in Fig. 5b. The improvement is mainly due to the enhanced light harvesting ability within the electrode when SrAl₂O₄:Eu,Dy is introduced.

As mentioned above, the important property associated with SrAl₂O₄:Eu,Dy is the emission of long persistent light. Therefore, after one sun illumination for 1 min, the light source was turned off and the photovoltaic performance of the cells containing the P25/SrAl₂O₄:Eu,Dy/CdS electrode was measured. Table 2 lists the corresponding data. It can be seen that the cells show an efficiency of 0.07% in the dark. Although the value is low, this novel concept is worthy of exploration because it could provide a possibility to fulfil the operation of solar cells in the dark if the long afterglow phosphor technology can be developed well in the future.

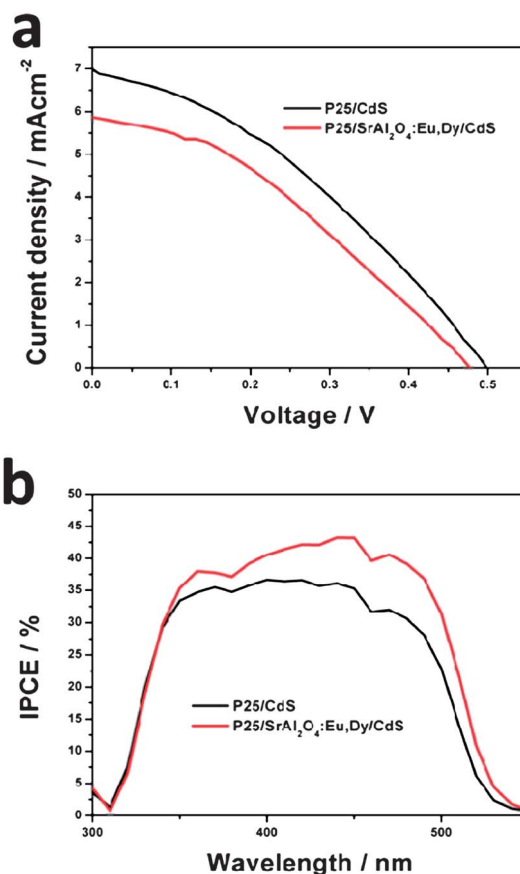


Fig. 5 (a) *J*–*V* curves for cells containing the P25/CdS and P25/SrAl₂O₄:Eu,Dy/CdS electrodes, (b) the corresponding IPCE curves.

Table 1 Photovoltaic parameters for the cells containing the P25/CdS and P25/SrAl₂O₄:Eu,Dy/CdS electrodes

Sample	<i>J</i> _{sc} /mA cm ^{−2}	<i>V</i> _{oc} /V	FF/%	η/%
P25/CdS	5.87	0.47	35.4	0.98
P25/SrAl ₂ O ₄ :Eu,Dy/CdS	7.07	0.50	35.3	1.24

Table 2 Photovoltaic parameters of cells containing the P25/SrAl₂O₄:Eu,Dy/CdS electrode in the dark after 100 mW cm^{−2} illumination for 1 min

Sample	<i>J</i> _{sc} /mA cm ^{−2}	<i>V</i> _{oc} /V	FF/%	η/%
P25/SrAl ₂ O ₄ :Eu,Dy/CdS	0.10	0.17	48.0	0.07

Conclusions

Long afterglow SrAl₂O₄:Eu,Dy phosphors were used on top of a transparent TiO₂ layer in CdS QDSSCs. Due to enhanced light harvesting abilities mainly *via* improved absorption and scattering, the as-prepared cells containing SrAl₂O₄:Eu,Dy achieved a conversion efficiency of 1.24% under one sun illumination, which is an increase of 26.5% compared with cells without

SrAl₂O₄:Eu,Dy (0.98%). After 100 mW cm⁻² illumination for 1 min, the light source was turned off. Cells containing SrAl₂O₄:Eu,Dy still show an efficiency of 0.07% in the dark due to the long afterglow properties of the SrAl₂O₄:Eu,Dy phosphors.

Notes and references

- 1 P. Ardalán, T. P. Brennan, H. B. R. Lee, J. R. Bakke, I. K. Ding, M. D. McGehee and S. F. Bent, *ACS Nano*, 2011, **5**, 1495.
- 2 Q. Zhang, G. Chen, Y. Yang, X. Shen, Y. Zhang, C. Li, R. Yu, Y. Luo, D. Li and Q. Meng, *Phys. Chem. Chem. Phys.*, 2012, **14**, 6479.
- 3 S. Q. Fan, B. Fang, J. H. Kim, J. J. Kim, J. S. Yu and J. Ko, *Appl. Phys. Lett.*, 2010, **96**, 063501.
- 4 P. Yu, K. Zhu, A. G. Norman, S. Ferrere, A. J. Frank and A. J. Nozik, *J. Phys. Chem. B*, 2006, **110**, 25451.
- 5 P. K. Santra and P. V. Kamat, *J. Am. Chem. Soc.*, 2012, **134**, 2508.
- 6 M. Samadpour, S. Giménez, A. I. Zad, N. Taghavinia and I. Mora-Seró, *Phys. Chem. Chem. Phys.*, 2012, **14**, 522.
- 7 G. Zhu, L. K. Pan, T. Xu and Z. Sun, *ACS Appl. Mater. Interfaces*, 2011, **3**, 3146.
- 8 T. L. Li, Y. L. Lee and H. Teng, *Energy Environ. Sci.*, 2012, **5**, 5315.
- 9 S. Y. Yang, A. S. Nair, R. Jose and S. Ramakrishna, *Energy Environ. Sci.*, 2010, **3**, 2010.
- 10 M. Grätzel, *Nature*, 2001, **414**, 338.
- 11 X. D. Li, D. W. Zhang, S. Chen, H. Zhang, Z. Sun, S. M. Huang and X. J. Yin, *Nano-Micro Lett.*, 2011, **3**, 195.
- 12 I. Chung, B. Lee, J. He, R. P. H. Chang and M. G. Kanatzidis, *Nature*, 2012, **485**, 486.
- 13 J. G. Radich, R. Dwyer and P. V. Kamat, *J. Phys. Chem. Lett.*, 2011, **2**, 2453.
- 14 J. Xu, X. Yang, T. L. Wong and C. S. Lee, *Nanoscale*, 2012, **4**, 6537.
- 15 A. Braga, S. Giménez, I. Concina, A. Vomiero and I. Mora-Seró, *J. Phys. Chem. Lett.*, 2011, **2**, 454.
- 16 A. Yella, H. W. Lee, H. N. Tsao, C. Yi, A. K. Chandiran, M. K. Nazeeruddin, E. W. G. Diau, C. Y. Yeh, S. M. Zakeeruddin and M. Grätzel, *Science*, 2011, **334**, 629.
- 17 J. H. Yum, E. Baranoff, S. Wenger, M. K. Nazeeruddin and M. Grätzel, *Energy Environ. Sci.*, 2011, **4**, 842.
- 18 Z. J. Ning, Y. Fu and H. Tian, *Energy Environ. Sci.*, 2010, **3**, 1170.
- 19 H. Sun, D. Qin, S. Huang, X. Guo, D. Li, Y. Luo and Q. Meng, *Energy Environ. Sci.*, 2011, **4**, 2630.
- 20 H. Sun, Y. Luo, Y. Zhang, D. Li, Z. Yu, K. Li and Q. Meng, *J. Phys. Chem. C*, 2010, **114**, 11673.
- 21 I. Robel, V. Subramanian, M. Kuno and P. V. Kamat, *J. Am. Chem. Soc.*, 2006, **128**, 2385.
- 22 M. Grätzel, *Inorg. Chem.*, 2005, **44**, 6841.
- 23 C. H. Chang and Y. L. Lee, *Appl. Phys. Lett.*, 2007, **91**, 053503.
- 24 C. Y. Chen, S. J. Wu, J. Y. Li, C. G. Wu, J. G. Chen and K. C. Ho, *Adv. Mater.*, 2007, **19**, 3888.
- 25 B. E. Hardin, E. T. Hoke, P. B. Armstrong, J. H. Yum, P. Comte, T. Torres, J. M. J. Fréchet, M. K. Nazeeruddin, M. Grätzel and M. D. McGehee, *Nat. Photonics*, 2009, **3**, 406.
- 26 B. Tan and Y. Wu, *J. Phys. Chem. B*, 2006, **110**, 15932.
- 27 H. Tian, E. Gabrielsson, Z. Yu, A. Hagfeldt, L. Kloo and L. Sun, *Chem. Commun.*, 2011, **47**, 10124.
- 28 A. Hagfeldt, G. Boschloo, L. Sun, L. Kloo and H. Pettersson, *Chem. Rev.*, 2010, **110**, 6595.
- 29 I. G. Yu, Y. J. Kim, H. J. Kim, C. Lee and W. I. Lee, *J. Mater. Chem.*, 2010, **21**, 532.
- 30 W. Shao, F. Gu, L. Gai and C. Li, *Chem. Commun.*, 2011, **47**, 5046.
- 31 J. Yang, L. K. Pan, G. Zhu, X. J. Liu, H. C. Sun and Z. Sun, *J. Electroanal. Chem.*, 2012, **677–680**, 101.
- 32 G. Zhu, L. K. Pan, J. Yang, X. J. Liu, H. C. Sun and Z. Sun, *J. Mater. Chem.*, 2012, **22**, 24326.
- 33 Y. Z. Zheng, X. Tao, L. X. Wang, H. Xu, Q. Hou, W. L. Zhou and J. F. Chen, *Chem. Mater.*, 2010, **22**, 928.
- 34 H. Wang, M. Miyauchi, Y. Ishikawa, A. Pyatenko, N. Koshizaki, Y. Li, L. Li, X. Li, Y. Bando and D. Golberg, *J. Am. Chem. Soc.*, 2011, **133**, 19102.
- 35 Y. C. Park, Y. J. Chang, B. G. Kum, E. H. Kong, J. Y. Son, Y. S. Kwon, T. Park and H. M. Jang, *J. Mater. Chem.*, 2011, **21**, 9582.
- 36 F. Huang, D. Chen, X. L. Zhang, R. A. Caruso and Y. B. Cheng, *Adv. Funct. Mater.*, 2010, **20**, 1301.
- 37 J. Wu, G. Xie, J. Lin, Z. Lan, M. Huang and Y. Huang, *J. Power Sources*, 2010, **195**, 6937.
- 38 Q. Li, J. Lin, J. Wu, Z. Lan, Y. Wang, F. Peng and M. Huang, *Electrochim. Acta*, 2011, **56**, 4980.
- 39 G. B. Shan, H. Assaoudi and G. P. Demopoulos, *ACS Appl. Mater. Interfaces*, 2011, **3**, 3239.
- 40 E. Klampaftis, D. Ross, K. R. McIntosh and B. S. Richards, *Sol. Energy Mater. Sol. Cells*, 2009, **93**, 1182.
- 41 J. de Wild, A. Meijerink, J. K. Rath, W. van Sark and R. E. I. Schropp, *Energy Environ. Sci.*, 2011, **4**, 4835.
- 42 H. Hafez, M. Saif and M. Abdel-Mottaleb, *J. Power Sources*, 2011, **196**, 5792.
- 43 G. Zhu, X. J. Wang, H. L. Li, L. K. Pan, H. C. Sun, X. J. Liu, T. Lv and Z. Sun, *Chem. Commun.*, 2012, **48**, 958.
- 44 T. Peng, L. Huajun, H. Yang and C. Yan, *Mater. Chem. Phys.*, 2004, **85**, 68.
- 45 S. Yesilay Kaya, E. Karacaoglu and B. Karasu, *Ceram. Int.*, 2012, **38**, 3701.
- 46 G. Zhu, L. K. Pan, T. Xu and Z. Sun, *ACS Appl. Mater. Interfaces*, 2011, **3**, 1472.
- 47 G. Zhu, L. K. Pan, T. Xu, Q. Zhao, B. Lu and Z. Sun, *Nanoscale*, 2011, **3**, 2188.
- 48 Y. L. Lee and C. H. Chang, *J. Power Sources*, 2008, **185**, 584.
- 49 T. Matsuzawa, Y. Aoki, N. Takeuchi and Y. Murayama, *J. Electrochem. Soc.*, 1996, **143**, 2670.
- 50 T. Y. Peng, H. P. Yang, X. L. Pu, B. Hu, Z. C. Jiang and C. H. Yan, *Mater. Lett.*, 2004, **58**, 352.
- 51 H. Yamamoto and T. Matsuzawa, *J. Lumin.*, 1997, **72–74**, 287.
- 52 I. n. Mora-Seró, S. Giménez, F. Fabregat-Santiago, R. Gómez, Q. Shen, T. Toyoda and J. Bisquert, *Acc. Chem. Res.*, 2009, **42**, 1848.
- 53 L. W. Chong, H. T. Chien and Y. L. Lee, *J. Power Sources*, 2010, **195**, 5109.